

Spectroscopic characterization of naturally and chemically oxidized silicon surfaces

Kazuaki Tsunoda, Emiko Ohashi, and Sadao Adachi^{a)}

Department of Electronic Engineering, Faculty of Engineering, Gunma University, Kiryu-shi, Gunma 376-8515, Japan

(Received 16 June 2003; accepted 29 July 2003)

We have determined the thicknesses of naturally and chemically grown oxides on HF-cleaned silicon surfaces in ambient air and in $\text{NH}_4\text{OH}/\text{H}_2\text{O}_2/\text{H}_2\text{O}$ solution, respectively, using spectroscopic ellipsometry. The naturally grown oxide thickness versus air-exposure time plots yield a rate constant of $3.5 \pm 0.5 \text{ \AA}/\text{decade}$ in ambient air. Chemical oxidation occurs immediately upon immersing the sample in the chemical solution and leaves the sample surface terminated with $\sim 6 \text{ \AA}$ of a chemical oxide. Photorefectance intensity is found to be strongly dependent on such surface processing, and results are explained by the different degree of surface (interface) states. © 2003 American Institute of Physics. [DOI: 10.1063/1.1613792]

I. INTRODUCTION

Wet chemical processing of semiconductors plays an essential role in the manufacture of many semiconductor devices. Prior to device processing, the single-crystalline silicon wafers must be cleaned and then passivated to protect against further contamination before the normal device processing starts. A wide variety of chemicals have been used for those purposes, but most processes share the common step of hydrofluoric acid (HF) etching to remove natural oxide from the silicon surface. The cleaning procedure that is also popularly used for silicon wafers is the so-called Radio Corporation of America (RCA) cleaning.^{1,2} This cleaning consists of two steps, commonly called SC1 and SC2. The SC1 step involves cleaning in $1\text{NH}_4\text{OH}/1\text{H}_2\text{O}_2/5\text{H}_2\text{O}$ at temperatures between 75 and 90 °C. The SC2 step consists of cleaning in a $1\text{HCl}/1\text{H}_2\text{O}_2/6\text{H}_2\text{O}$ solution at 70–90 °C.

The physical and chemical properties of HF-cleaned silicon surfaces have been extensively studied by various authors using Fourier-transform infrared spectroscopy (FTIR), x-ray photoelectron spectroscopy (XPS), scanning tunneling microscopy (STM), etc.³ The uniformity of an oxide film formed on silicon surface by RCA processing has been investigated using STM by Aoyama *et al.*⁴ The structure of surface oxides formed in various chemical solutions, including RCA, has also been studied using glancing incidence x-ray reflectometry and FTIR by Sugita *et al.*⁵ and using XPS, transmission electron microscopy, and FTIR by Ohwaki *et al.*⁶

The purpose of this article is to study the effects of HF and SC1 treatments on the surface properties of silicon wafers using spectroscopic ellipsometry (SE) and photorelectance (PR) spectroscopy. SE is a very surface-sensitive technique, which enables detection of submonolayer coverage of the surface by adsorbed species.⁷ PR is a contactless form of electroreflectance, in which reflectance modulation is produced by a chopped exciting light beam. It can yield sharp

critical-point structures and also be very sensitive to surface or interface.⁸ However, no detailed study has been performed on surface properties of silicon by using SE and PR techniques. We determine rate constants of the natural and chemical oxide growths on HF-cleaned silicon surfaces exposed to air and immersed in the SC1 solution, respectively, using SE. We also investigate the passivation effects of these natural and chemical oxides by measuring PR spectra. It is shown that the PR intensity is strongly dependent on surface processing conditions. The fact can be explained by the different degree of surface or interface states on such processed sample surfaces.

II. EXPERIMENT

We used *n*-type Si(110) wafers with a resistivity of 0.010–0.018 $\Omega \text{ cm}$ ($N_D \sim 3 \times 10^{18} \text{ cm}^{-3}$). They were degreased with organic solutions in an ultrasonic bath. The samples were then etched in a 1.5% HF solution at room temperature and rinsed in a de-ionized (DI) water. The composition of the SC1 solution is $\text{NH}_4\text{OH}:\text{H}_2\text{O}_2:\text{H}_2\text{O}$ in a volume ratio of 1:1:5. The samples were put in a bath of SC1 solution at 80 °C, followed by rinsing with DI water. As we will see later, the SC1 treatment causes in chemical oxidation of silicon surfaces.

The automatic ellipsometer used was of the polarizer–sample–rotating–analyzer type. SE measurements were carried out in the 1.2–5.2 eV photon-energy range at room temperature. The angle of incidence and the polarizer azimuth were set at 70° and 45°, respectively. The experimental setup for PR measurement was essentially the same as that described in the literature.⁹ The 488 nm line of an Ar^+ laser chopped at 325 Hz was used as the pumping light. The probe light from a 150 W xenon lamp was irradiated near to normal on the sample surface. The PR spectra were measured in the 2.9–4.0 eV photon-energy range at room temperature using a grating spectrometer (JASCO CT-25C) and a thermoelectrically cooled photomultiplier tube (Hamamatsu R375).

^{a)}Electronic mail: adachi@el.gunma-u.ac.jp

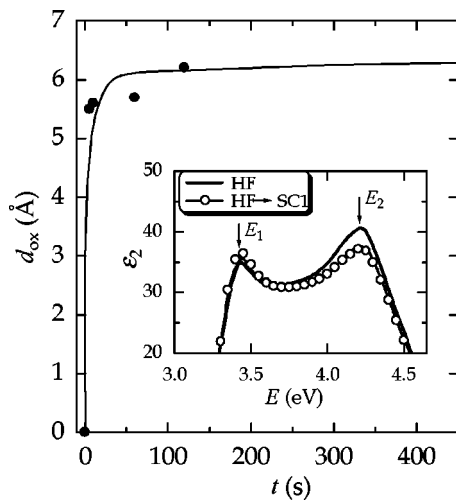


FIG. 1. Plots of the chemical oxide thickness d_{ox} on Si(100) surface vs immersion time t in the SC1 solution at 80 °C. The thickness d_{ox} is estimated from a simple three-layer (ambient/SiO₂/silicon) model. The inset shows the fitted result of this model for sample etched in 1.5% HF solution, followed by SC1 treatment for $t=120$ s. For comparison, the HF-cleaned $\varepsilon(E)$ spectrum is shown by the heavy solid line.

III. RESULTS AND DISCUSSION

The SE measurement can be used to yield direct information about the relative quality of surface regions prepared by different methods.⁷ Figure 1 shows the plots of the chemical oxide thickness d_{ox} on Si(100) surface versus immersion time t in the SC1 solution at 80 °C. The oxide thickness d_{ox} was determined from Fresnel's formula using a three-layer (ambient/chemical oxide layer/bulk silicon) model. An example of this analysis is shown in the inset of Fig. 1. There have been no experimental data on the optical constants of the chemical oxide. We, therefore, used here those of silicon dioxide (SiO₂). Thus, the d_{ox} values plotted here are the effective oxide thicknesses, not the real ones. The SE $\varepsilon(E)$ data of the HF-cleaned surface are also used as those for the bulk silicon. The fit shown in the inset of Fig. 1 gives the effective oxide thickness of about 6 Å.

The d_{ox} vs t plots in Fig. 1 suggest that the chemical oxidation occurs immediately upon immersing the sample in the SC1 solution. It is also understood that the effective oxide thickness d_{ox} shows a saturated value of about 6 Å. This value is in good agreement with those reported in the literature (6–10 Å).^{10–12} We also found no clear difference in the chemical oxidation properties among the Si(100), (110), and (111) surfaces.

The SE technique is also used to study the activity of freshly HF-etched Si(110) surfaces in ambient air. The time dependence of the natural oxide thickness d_{ox} usually shows a logarithmic behavior given by

$$d_{\text{ox}} = d_0 \log\left(\frac{t}{t_0}\right). \quad (1)$$

The solid line in Fig. 2 represents the calculated result of this expression. The slope d_0 is ~ 3.5 Å/decade. This value is much smaller than 6.8 Å/decade as measured by Archer¹³ on polished surface of unknown orientation, but is in good

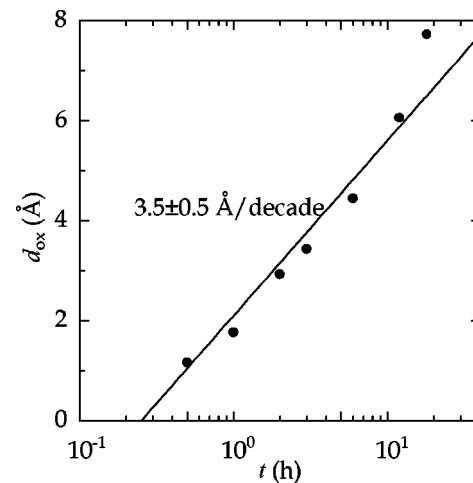


FIG. 2. Native oxide thickness d_{ox} on HF-cleaned Si(110) surface vs air-exposure time t .

agreement with that on Si(100) surface (~ 4 Å/decade) reported by Hirose *et al.*¹⁴ We also found that the rate value d_0 is nearly the same among the HF-cleaned Si(100), (110), and (111) surfaces (3.5 ± 0.5 Å/decade).

Figure 3 shows the PR spectra for n -Si(110) samples taken after four different surface processing: (a) degreased in organic solvents, (b) degreased in organic solvents and then etched in a 1.5% HF solution at 20 °C for 120 s, (c) degreased, 1.5% HF etched, and finally SC1 treated at 80 °C for 120 s, and (d) degreased, 1.5% HF-etched, and then air-exposed about 12 h. Note that samples (a) and (d) have the natural oxide overlayers of about 13 and 6 Å thicknesses,

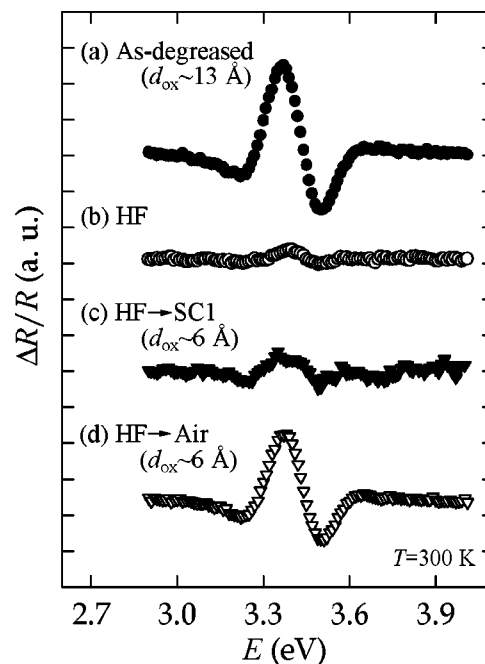


FIG. 3. PR spectra for n -Si(110) samples taken after four different surface processing: (a) degreased in organic solvents, (b) degreased in organic solvents and then etched in a 1.5% HF solution at 20 °C for 120 s, (c) degreased, 1.5% HF-etched, and finally SC1-treated at 80 °C for 120 s, and (d) degreased, 1.5% HF-etched, and then air-exposed about 12 h.

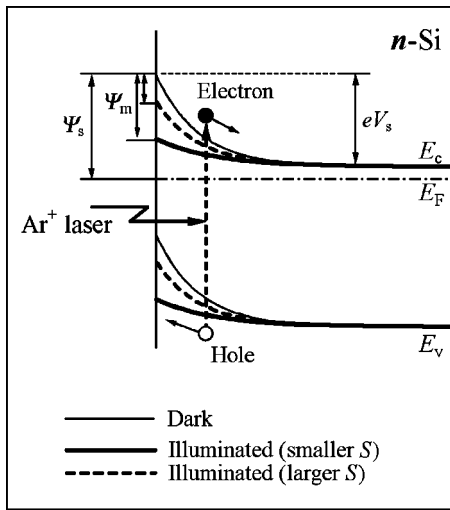


FIG. 4. Schematic energy-band configuration in the vicinity of the surface of an *n*-type silicon with and without pumping light (Ar^+ laser) illumination. The cases for the smaller and larger surface recombination velocities (S 's) are shown by the heavy solid and dashed lines, respectively.

respectively, and sample (c) has the chemical oxide overlayer of about 6 Å thickness. Sample (b) has no or a very thin natural oxide overlayer.

The dominant peak seen in the 3–4 eV region of PR spectrum is due to the E_1 transitions. The E_1 transitions occur along the $\langle 111 \rangle$ direction or at the L point in the Brillouin zone. It is evident that the PR intensity is strongly dependent on the surface chemical treatment used. The strongest PR intensity is observed from the as-degreased sample [(a)], while the weakest signal is from the sample just after being etched in the 1.5% HF solution [(b)]. It is also noteworthy to point out that samples (c) and (d) have nearly the same oxide thicknesses (~ 6 Å); however, their PR intensities differ significantly.

The schematic energy-band configuration in the vicinity of the surface of an *n*-type silicon with and without light illumination is shown in Fig. 4. The photoexcited carriers are separated by the electric field in the surface space-charge layer, with electrons and holes drifting into opposite directions. Excess minority holes, that move toward the surface, lead to a redistribution of the equilibrium space charge and consequently to a change in band bending. The resulting change in surface potential Ψ_m affects the PR intensity. Note that $|\Delta R/R|$ is proportional to the square of the surface electric field.¹⁵ The square of the electric field is also proportional to surface potential. Consequently, $|\Delta R/R|$ is proportional to Ψ_m .¹⁶

The surface recombination velocity S may be the only parameter required to characterize the surface.¹⁷ Minority carriers are annihilated there by recombination via surface states. The larger the surface recombination velocity S , the smaller the minority carrier accumulation. Thus, we can expect that the smaller the surface recombination velocity, the larger the surface potential change Ψ_m (see Fig. 4). Therefore, the PR intensity is largely dependent on the surface processing conditions, as clearly observed in Fig. 3.

The photomodulated surface potential Ψ_m can be deter-

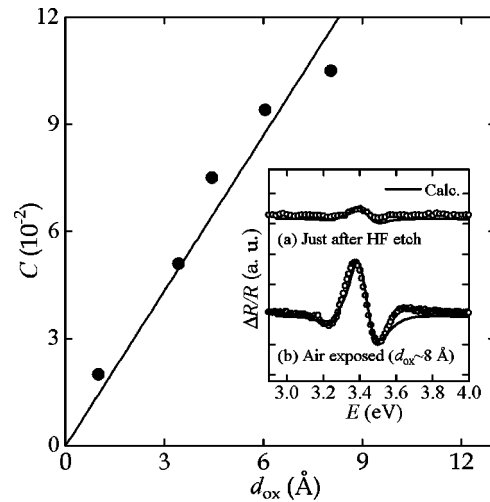


FIG. 5. E_1 -edge strength parameter C plotted as a function of natural oxide thickness d_{ox} on HF-cleaned Si(110) surface. The thickness d_{ox} is determined by SE. The parameter C is derived from the standard critical-point fit. Examples of this fit are shown in the inset.

mined by the steady-state condition of the photogenerated carriers at the surface space-charge region. The thickness of the surface space-charge region W can be given by

$$W = \left(\frac{2\epsilon_0\epsilon_s V_s}{eN_D} \right)^{1/2}, \quad (2)$$

where ϵ_s is the relative dielectric constant, ϵ_0 is the dielectric permittivity of vacuum, e is the elementary charge, V_s is the barrier height at the surface (see Fig. 4), and N_D is the donor concentration. It is not easy to determine the surface barrier height V_s from the PR spectra measured in the opaque region. Assuming $V_s = 0.5$ V and putting $\epsilon_s = 11.6$ and $N_D \sim 3 \times 10^{18} \text{ cm}^{-3}$ into Eq. (2), we obtain $W \sim 15$ nm. The surface space-charge width W is, thus, much smaller than the minority-hole diffusion length in *n*-type silicon¹⁸ and also smaller than the penetration depth (~ 500 nm) of the pumping light.¹⁹ Differences in the PR intensity observed in Fig. 3 are, indeed, due to surface effect.

We can expect from Fig. 3 that the PR intensity of the HF-etched sample will increase with increasing air-exposure time. This is because the HF-etched surface will be passivated with a gradual growth of the natural oxide on it. Figure 5 plots the PR strength parameter C vs d_{ox} measured on the 1.5% HF-cleaned Si(110) surface after exposing in air for various times. The PR strength parameter C is determined from the fit using the standard critical-point line shape²⁰

$$\frac{\Delta R}{R} = \text{Re} \left[\sum_{j=1}^p C_j e^{i\theta_j} (E - E_{gj} + i\Gamma_j)^{-n_j} \right], \quad (3)$$

where p is the number of the spectral functions to be fitted and θ is the phase angle. The power term n refers to the type of optical transitions in question: $n = 2, 2.5,$ and 3 for an exciton, a three-dimensional one-electron transition, and a two-dimensional one-electron transition, respectively. Because $|\Delta R/R|$ is proportional to Ψ_m , C is also proportional to Ψ_m . We considered here not only the dominant E_1 transitions at 3.41 eV, but also those at $E'_0 = 3.27$ eV, $E_2(X)$

=4.31 eV, and $E_2(\Sigma)=4.55$ eV (i.e., $p=4$).²⁰ The parameter C is fit determined by keeping $n=3$ and using constant values of θ and Γ . Examples of this fit are shown in the inset of Fig. 5.

It is clear from Fig. 5 that an increase in air-exposure time results in an increase in the PR intensity. It is also clear from Fig. 3 that the SC1-formed chemical oxide does not effectively passivate the HF-cleaned silicon surface. It has been reported⁵ that the chemical oxide contains many silicon hydrides and oxyhydrides and that the amounts of these hydrides depend on the chemical solutions used. Low density and chemical imperfections have also been found in oxides formed in chemical solutions, such as $\text{NH}_4\text{OH}/\text{H}_2\text{O}_2$ (SC1) and $\text{HCl}/\text{H}_2\text{O}_2$ (SC2).

IV. CONCLUSIONS

In summary, we have determined the thicknesses of natural and chemical oxides grown on silicon surfaces in ambient air and in the SC1 solution, respectively, using SE. The PR intensity is also found to be strongly dependent on the surface treatment used; the strongest PR intensity is obtained on the as-degreased surface, while the weakest intensity is observed from the sample just after etched in the 1.5% HF solution. The surface covered with the chemical oxide also gives very weak PR intensity. These results can be interpreted by the different minority-carrier recombination velocities at the surface (interface), i.e., the smaller the surface recombination velocity, the larger the surface potential change Ψ_m . Further study needs to make clear the electronic

structure of the natural (chemical) oxide/silicon interfaces and its correlation with PR intensity.

- ¹W. Kern and D. Puotinen, *RCA Rev.* **31**, 187 (1970).
- ²W. Kern, *RCA Rev.* **31**, 207 (1970).
- ³See, for example, T. Konishi, K. Uesugi, K. Takaoka, S. Kawano, M. Yoshimura, and T. Yao, *Jpn. J. Appl. Phys., Part 1* **32**, 3131 (1993).
- ⁴T. Aoyama, T. Yamazaki, and T. Ito, *Appl. Phys. Lett.* **61**, 102 (1992).
- ⁵Y. Sugita, S. Watanabe, and N. Awaji, *Jpn. J. Appl. Phys., Part 1* **35**, 5437 (1996), and references therein.
- ⁶T. Ohwaki, M. Takeda, and Y. Takai, *Jpn. J. Appl. Phys., Part 1* **36**, 5507 (1997).
- ⁷D. E. Aspnes and A. A. Studna, *Appl. Phys. Lett.* **39**, 316 (1981).
- ⁸F. H. Pollak, in *Handbook on Semiconductors*, edited by M. Balkanski (North-Holland, Amsterdam, 1994), Vol. 2, p. 527.
- ⁹R. N. Bhattacharya, H. Shen, P. Parayanthal, F. H. Pollak, T. Coutts, and H. Aharoni, *Phys. Rev. B* **37**, 4044 (1988).
- ¹⁰A. Philipossian, *J. Electrochem. Soc.* **139**, 2956 (1992).
- ¹¹T. Ohwaki, M. Takeda, and Y. Takai, *Jpn. J. Appl. Phys., Part 1* **36**, 5507 (1997).
- ¹²G. K. Celler, D. L. Barr, and J. M. Rosamilia, *Electrochem. Solid-State Lett.* **3**, 47 (2000).
- ¹³R. J. Archer, *J. Electrochem. Soc.* **104**, 619 (1957).
- ¹⁴M. Hirose, T. Yasaka, and S. Miyazaki, in *Handoutai Kenkyu*, edited by J. Nishizawa (Kogyo Chosakai, Tokyo, 1992), Vol. 36, p. 263 (in Japanese).
- ¹⁵D. E. Aspnes, *Surf. Sci.* **37**, 418 (1967).
- ¹⁶A. Fujimoto, H. Katsumi, M. Okuyama, and Y. Hamakawa, *Jpn. J. Appl. Phys., Part 1* **34**, 804 (1995).
- ¹⁷V. Grivickas, J. A. Tellefsen, and M. Willander, in *Properties of Crystalline Silicon*, EMIS Datareviews Series No. 20, edited by R. Hull (INSPEC, London, 1999), p. 718.
- ¹⁸J. A. del Alamo, in *Properties of Silicon*, EMIS Datareviews Series No. 4 (INSPEC, London, 1988), p. 164.
- ¹⁹S. Adachi, *Optical Constants of Crystalline and Amorphous Semiconductors: Numerical Data and Graphical Information* (Kluwer Academic, Boston, 1999).
- ²⁰H. Moriya, A. Kaneta, and S. Adachi, *Mater. Sci. Eng., B* **76**, 232 (2000).